Geophysical Research Letters

RESEARCH LETTER
10.1029/2023GL103509

Drift of Earth's Pole Confirms Groundwater Depletion as a Significant Contributor to Global Sea Level Rise 1993–2010

Ki-Weon Seo[1,2], Dongryeol Ryu[3], Jooyoung Eom[4], Taewhan Jeon[2], Jae-Seung Kim[1], Kookhyoun Youm[1], Jianli Chen[5,6], and Clark R. Wilson[7,8]

[1]Department of Earth Science Education, Seoul National University, Seoul, Republic of Korea, [2]Center for Educational Research, Seoul National University, Seoul, Republic of Korea, [3]Department of Infrastructure Engineering, The University of Melbourne, Parkville, VIC, Australia, [4]Department of Earth Science Education, Kyungpook National University, Daegu, Republic of Korea, [5]Department of Land Surveying and Geo-informatics, Hong Kong Polytechnic University, Hong Kong, China, [6]Research Institute for Land and Space, The Hong Kong Polytechnic University, Hong Kong, China, [7]Department of Geological Sciences, Jackson School of Geosciences, University of Texas at Austin, Austin, TX, USA, [8]Center for Space Research, University of Texas at Austin, Austin, TX, USA

Key Points:

- Earth's pole has drifted toward 64.16°E at a speed of 4.36 cm/yr during 1993–2010 due to groundwater depletion and resulting sea level rise
- Including groundwater depletion effects, the estimated drift of Earth's rotational pole agrees remarkably well with observations

Supporting Information:

Supporting Information may be found in the online version of this article.

Correspondence to:

K.-W. Seo,
seokiweon@snu.ac.kr

Citation:

Seo, K.-W., Ryu, D., Eom, J., Jeon, T., Kim, J.-S., Youm, K., et al. (2023). Drift of Earth's pole confirms groundwater depletion as a significant contributor to global sea level rise 1993–2010. *Geophysical Research Letters*, *50*, e2023GL103509. https://doi.org/10.1029/2023GL103509

Received 2 MAR 2023
Accepted 9 MAY 2023

Author Contributions:

Conceptualization: Ki-Weon Seo, Taewhan Jeon
Data curation: Ki-Weon Seo, Kookhyoun Youm
Formal analysis: Ki-Weon Seo, Kookhyoun Youm
Funding acquisition: Ki-Weon Seo
Investigation: Ki-Weon Seo, Jooyoung Eom
Methodology: Ki-Weon Seo, Dongryeol Ryu, Jae-Seung Kim
Software: Ki-Weon Seo
Supervision: Clark R. Wilson
Visualization: Jooyoung Eom, Taewhan Jeon

Abstract Climate model estimates show significant groundwater depletion during the 20th century, consistent with global mean sea level (GMSL) budget analysis. However, prior to the Argo float era, in the early 2000's, there is little information about steric sea level contributions to GMSL, making the role of groundwater depletion in this period less certain. We show that a useful constraint is found in observed polar motion (PM). In the period 1993–2010, we find that predicted PM excitation trends estimated from various sources of surface mass loads and the estimated glacial isostatic adjustment agree very well with the observed. Among many contributors to the PM excitation trend, groundwater storage changes are estimated to be the second largest (4.36 cm/yr) toward 64.16°E. Neglecting groundwater effects, the predicted trend differs significantly from the observed. PM observations may also provide a tool for studying historical continental scale water storage variations.

Plain Language Summary Melting of polar ice sheets and mountain glaciers has been understood as a main cause of sea level rise associated with contemporary climate warming. It has been proposed that an important anthropogenic contribution is sea level rise due to groundwater depletion resulting from irrigation. A climate model estimate for the period 1993–2010 gives total groundwater depletion of 2,150 GTon, equivalent to global sea level rise of 6.24 mm. However, direct observational evidence supporting this estimate has been lacking. In this study, we show that the model estimate of water redistribution from aquifers to the oceans would result in a drift of Earth's rotational pole, about 78.48 cm toward 64.16°E. In combination with other well-understood sources of water redistribution, such as melting of polar ice sheets and mountain glaciers, good agreement with PM observations serves as an independent confirmation of the groundwater depletion model estimate.

1. Introduction

Sea level rise is one of the most significant phenomena associated with the warming climate. Contemporary sea level rise has been monitored extensively by multiple observational techniques. For example, in the period 2005–2015, satellite altimetry showed global mean sea level (GMSL) rising at a rate of 3.5 mm/yr. Data from the Argo float network show that ocean density changes contributed about 1.3 mm/yr in steric GMSL rise (WCRP, 2018). The remainder (3.5–1.3 mm/yr = 2.2 mm/yr) is caused by ocean mass increase as confirmed by GRACE (Kim et al., 2019). GRACE also provides estimates of separate ocean mass contributions to GMSL rise associated with the Greenland ice sheet (GrIS), Antarctic ice sheet (AIS), mountain glaciers and terrestrial water storage (TWS). The TWS contribution has in the past been mistakenly understood as a contributor to GMSL decrease (Reager et al., 2016) because variations in Earth center of mass (geocenter) were not properly accounted for in GRACE data processing (Jeon et al., 2018). With proper consideration of geocenter motion, TWS change is recognized as a significant contributor to GMSL rise, ~0.3 mm/yr (Kim et al., 2019). TWS mainly includes contributions from artificial reservoirs behind dams, soil moisture and groundwater. The increasing number of dams and corresponding water storage increase have mitigated GMSL rise since the early 20th century. Therefore,

Writing – original draft: Ki-Weon Seo, Jae-Seung Kim, Jianli Chen, Clark R. Wilson
Writing – review & editing: Ki-Weon Seo, Dongryeol Ryu, Jianli Chen, Clark R. Wilson

contributions of TWS to GMSL rise inferred from GRACE data would be likely associated with declines in soil moisture and/or groundwater.

Prior to the GRACE mission, limited in situ and remote sensing data indicated that increasing storage in artificial reservoirs behind dams was a source of GMSL decrease, while melting ice from AIS, GrIS and mountain glaciers contributed to GMSL rise (Chao et al., 2008). Groundwater depletion simulated by climate models has been identified as a significant contributor to GMSL rise during the 20th century (Wada et al., 2010), but the limited availability of in situ or remote sensing groundwater data has left observational evidence lacking. Alternatively, the contribution of groundwater depletion to GMSL has been understood by examining time series of altimetric observations of GMSL. For example, Dieng et al. (2017) compared the observed GMSL rate and an estimated rate obtained from all known contributions to GMSL including anthropogenic sources (dam and groundwater effects) with a rate of 0.12 mm/yr for 1993–2015. Considering the effect of GMSL decrease due to impounding water behind dams, a positive GMSL contribution from anthropogenic effects is mostly associated with groundwater depletion (Chao et al., 2008). Agreement between observed and estimated GMSL rates provides evidence of global groundwater depletion and GMSL rise. However, analysis ought to include steric sea level changes which are highly uncertain prior to the Argo float era, beginning in 2005, when measurements for estimating steric effects to 2,000-m depth became available (Chen, Wilson, & Tapley, 2013). Dieng et al. (2017) showed that in the period 1993–2015, steric contributions to GMSL rise were in the range 0.90–1.70 mm/yr, a range that exceeds the likely groundwater contribution of ∼0.30 mm/yr.

Independent constraints on water mass redistribution are provided by polar motion (PM), variations in the position of Earth's rotational pole relative to the crust. Groundwater and other surface mass redistribution sources (including mountain glaciers, water stored in artificial reservoirs, AIS and GrIS mass changes, and soil moisture) all affect PM. PM is driven by degree-2 order 1 spherical harmonic changes in Earth's gravity field as well as atmospheric winds and ocean currents, with no contribution from steric sea level change. Therefore, both GRACE satellite gravity data and PM provide constraints on the magnitude and geographical distribution of groundwater depletion, assuming that good estimates of other contributors are available. Changes in Earth's dynamic oblateness (degree 2- order 0, or J_2) might also help constrain water mass redistribution, but J_2 is found to be relatively insensitive to groundwater depletion (see Section 4).

This study reviews the budget of GMSL in the period 1993–2010 using data and models for various hydrologic sources. We use associated PM predictions and observations to understand groundwater depletion estimates from a climate model. The study period was selected considering availability of both observations and model estimates.

2. Materials and Methods

Figures 1a and 1b show AIS and GrIS contributions to GMSL rise, respectively. Two different estimates are available during the study period. Red lines are based on a mass flux method that incorporates radar remote sensing of ice discharge and climate models for surface mass balance (Mouginot et al., 2019; Rignot et al., 2019). Blue lines are from the Ice sheet Mass Balance Inter-comparison Exercise (IMBIE) (The IMBIE Team, 2018, 2020) that combines various remote sensing and regional climate models over both ice sheets. Flux estimates show larger AIS and GrIS contributions to GMSL rise relative to IMBIE. Mountain glacier mass changes have been estimated by glaciologic and geodetic observations since the early 20th century. We show the three recent estimates of Xu and Chao (2019) (blue), Marzeion et al. (2015) (black), and Zemp et al. (2019) (red) in Figure 1c.

Contributions of three main TWS components to GMSL change are shown in Figures 1d–1f. These include variations in soil moisture (including snow water, a minor component) (Rodell et al., 2004), impounded water behind dams (Lehner et al., 2011) and groundwater (Wada et al., 2010), respectively. The soil moisture contribution shows pronounced inter-annual variations but little trend over time. Dams are an important cause of GMSL decrease. The impounded water in artificial reservoirs was estimated from a global database including locations, maximum capacities and construction completion times for 7,320 dams with cumulative capacity of about 7,000 km^3 since 1900. Seepage effects have also been included here. The first year of the seepage effect after impoundment was assumed to be 5% of the initial maximum capacity and it grows slowly proportional to square root of time (Chao et al., 2008). Groundwater depletion was derived using groundwater recharge and abstraction computed by the global hydrological model PCR-GLOBWB (Wada et al., 2010, 2011). Groundwater abstraction is based on a groundwater withdrawal and irrigated areas database around the year 2000. Groundwater abstraction of the

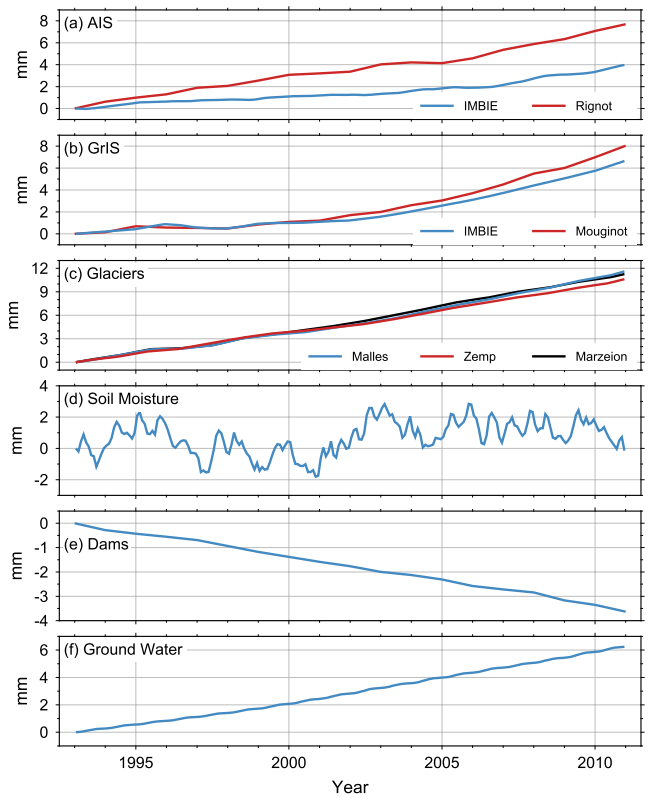

Figure 1. Global mean sea level (GMSL) contributions from the Antarctic ice sheet (AIS) (a), Greenland ice sheet (GrIS) (b), mountain glaciers (c), soil moisture (d), artificial reservoirs behind dams (e) and groundwater (f). Note differences in the vertical scales.

benchmark year 2000 was extended to other periods using net groundwater demand estimates (considering surface freshwater availability) simulated by PCR-GLOBWB. Groundwater variations have a relatively large effect on GMSL rise.

Using terrestrial water and ice mass change data described above, sea level variations were estimated based on mass conservation between land and oceans considering self-attraction and loading (SAL) effects (Jeon et al., 2018). Figure 2a shows total groundwater depletion during the analysis period, 1993–2010. Northwestern India and western North America show significant decreases in groundwater storage (Figure 2a). Most of the world's oceans experience an increase of near 10 mm, but a sea level drop over the Indian and the Pacific Ocean adjacent to regions of groundwater depletion (Figure 2b) is a consequence of SAL that causes sea level to decrease near regions of diminished water mass on land.

Changes in terrestrial water (σ_L) (e.g., Figure 2a) and oceanic (σ_O) (Figure 2b) mass loads were converted to spherical harmonic (SH) coefficients of the geoid:

$$\sigma_L(\theta,\lambda)+\sigma_O(\theta,\lambda)= \frac{a\rho_w}{3}\sum_{l=0}^{N}\sum_{m=0}^{l}\frac{1+k_l}{2l+1}\overline{P_{lm}}(\sin\theta)\left[\overline{C_{lm}}\cos(m\theta)+\overline{S_{lm}}\sin(m\theta)\right] \quad (1)$$

where $a\rho_w$ is the Earth radius times water density, (θ,λ) are latitude and longitude, $\overline{P_{lm}}$ are normalized associated Legendre polynomials and k_l are load Love numbers. Using the combined mass fields, $\sigma_L(\theta,\lambda)+\sigma_O(\theta,\lambda)$, PM excitations ($\chi_1$, χ_2) were computed from the degree 2 ($l=2$) order 1 ($m=1$) SH coefficients via (Chao, 1985; Seo et al., 2021):

$$\chi_1 = -\frac{\frac{\mathrm{Ma}^2\sqrt{5/3}}{(C-A)}}{1-1.551\times10^{-9}\frac{\mathrm{Ma}^2\sqrt{5/3}}{(C-A)}}\overline{C_{21}} \quad (2)$$

$$\chi_2 = -\frac{\frac{\mathrm{Ma}^2\sqrt{5/3}}{(C-A)}}{1-1.505\times10^{-9}\frac{\mathrm{Ma}^2\sqrt{5/3}}{(C-A)}}\overline{S_{21}}$$

in which M is the Earth mass, and C and A are Earth principal moments of inertia. χ_1 and χ_2 from Equation 2 include effects of rotational feedback. We then estimated monthly (χ_1, χ_2) changes from groundwater (storage on land and associated sea level change) plus the other sources (AIS, GrIS, glaciers, dams and soil moisture). χ_1 and χ_2 are mostly determined by terrestrial storage changes with minor contributions from corresponding sea level rise due to relatively uniform distribution of ocean mass as shown in Figure 2b. Contributions of sea level change

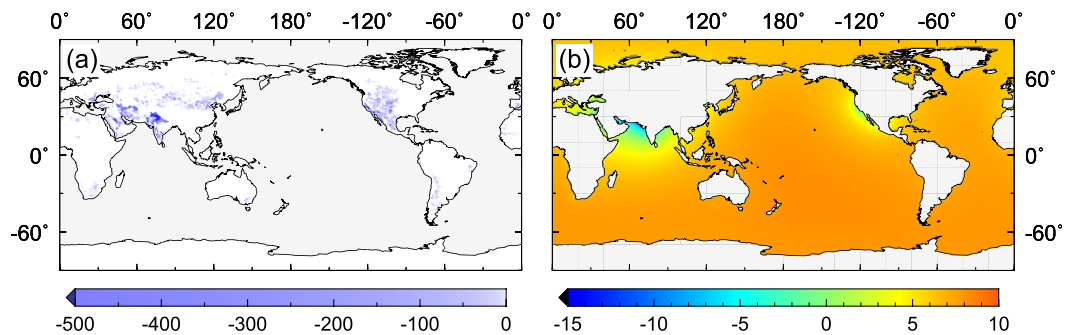

Figure 2. Total groundwater storage change on land (a) and the associated sea level variation (b) for 1993–2010. Units are mm of water.

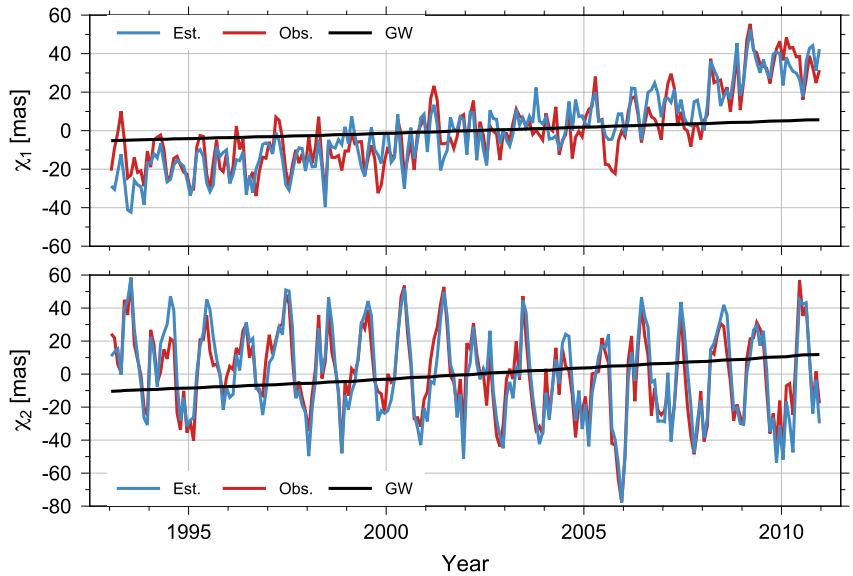

Figure 3. χ_1 (a) and χ_2 (b) variations for 1993–2010. Red lines are observed PM excitation (χ_1, χ_2) and blue lines are estimated from all known sources shown in blue lines in Figure 1. Barometric pressure, ocean bottom pressure, atmospheric wind and ocean current contributions are also included. Black lines show estimated PM excitation due to groundwater depletion.

resulting from terrestrial water and ice variations to χ_1 and χ_2 are estimated to be about 20.81% and 25.17% of total variance, respectively.

Additionally, we estimated (χ_1, χ_2) associated with barometric pressure (Hersbach et al., 2020), ocean bottom pressure (Köhl, 2020), atmospheric winds (Hersbach et al., 2020) and ocean currents (Köhl, 2020). These changes should not have notable contributions to trends in GMSL, but are an important source of PM excitation (χ_1, χ_2) at seasonal and shorter time scales.

GIA Models (e.g., Peltier et al., 2018) provide predictions of the GIA contribution to (χ_1, χ_2) but there is some variation among model estimates. Recently a new GIA estimate has been obtained by combining GRACE and PM observations (Seo et al., 2021). We used this result, as well as predictions from models of Peltier et al. (2018) and Caron et al. (2018).

3. Results

We first compare time series of PM excitation (χ_1, χ_2) from observations with estimates from all known sources of PM excitations. Red lines in Figure 3 show the two components χ_1 and χ_2 from observations (Bizouard et al., 2019) from 1993 to 2010. The dominant Chandler wobble resonance was mostly removed using a digital filter (Wilson, 1985). The International Earth Rotation Service (https://www.iers.org) provides various PM series, and we used the longest, EOP C01 IAU2000. χ_1 and χ_2 are in milliarcsecond (mas) along the Greenwich meridian and 90° east longitude, respectively. Blue lines show estimated (χ_1, χ_2) from all known sources of GMSL change shown in Figure 1, and effects of barometric pressure, ocean bottom pressure, winds and currents. Because we considered two estimates of polar ice sheet contributions, and three for mountain glaciers, six different estimates of (χ_1, χ_2) are possible for each GIA PM estimate. The estimate associated with blue lines shown in Figure 1 uses AIS and GrIS mass changes from IMBIE (The IMBIE Team, 2018, 2020) and mountain glacier mass changes from the most recent estimate (Xu & Chao, 2019) as well as soil moisture (Rodell et al., 2004), impounded water behind dams (Lehner et al., 2011) and groundwater (Wada et al., 2010). Effects of barometric pressure (Hersbach et al., 2020), ocean bottom pressure (Köhl, 2020), winds (Hersbach et al., 2020) and currents (Köhl, 2020) were also included. Each PM excitation contribution is shown in Supporting Information S1 (Figure S1). Most high frequency variations in (χ_1, χ_2) are explained by changes in barometric pressure, ocean bottom pressure, winds and currents. PM excitation variations associated with ice mass loss from mountain glaciers and Greenland show directional changes in PM excitation similar to previous studies around 1998 (Deng et al., 2021) and 2005 (Chen, Wilson, Ries, & Tapley, 2013), respectively.

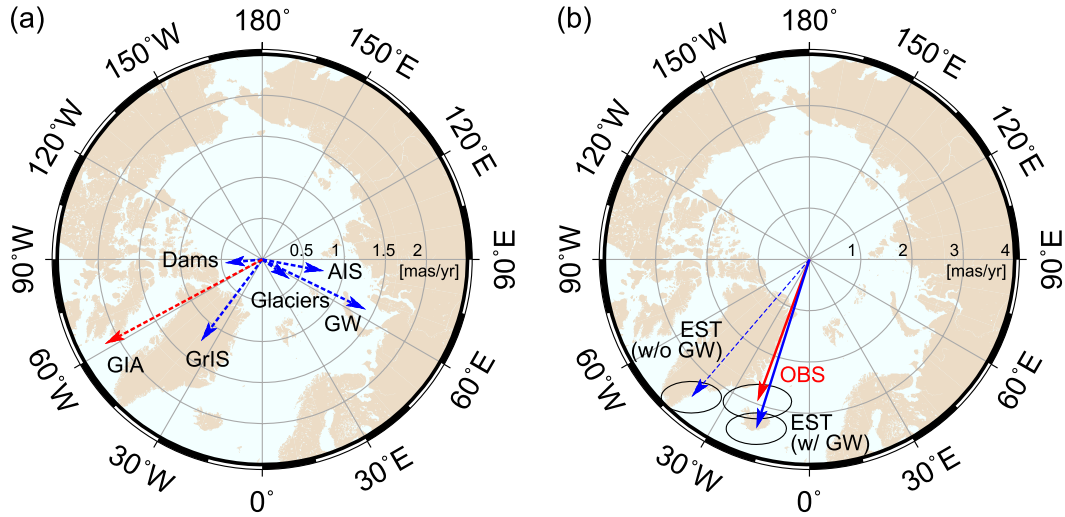

Figure 4. (a) Individual contributors to the PM excitation trend. (b) Sum of PM excitation trend contributors with (solid blue) and without (dashed blue) groundwater depletion. Red arrow is the observed PM excitation.

Figure 3 clearly shows that estimated and observed (χ_1, χ_2) agree well with each other. χ_1 shows a positive trend (Figure 3a) and χ_2 a small negative trend (Figure 3b), likely due both to GIA and contemporary surface mass redistribution (Adhikari & Ivins, 2016; Chen, Wilson, Ries, & Tapley, 2013). If groundwater (shown in black lines) were neglected, the estimated trend in χ_2 would disagree with the observed value (see Figure 4 in detail).

The importance of groundwater contributions to the rise in GMSL from 1993 to 2010 can be seen more clearly in a polar plot (Figure 4), which shows both magnitude and direction of trends. Each contribution from blue lines in Figure 1 is displayed in Figure 4a. Minor contributions to (χ_1, χ_2) trends from soil moisture, barometric pressure, ocean bottom pressure, winds and currents are not included. The red arrow shows GIA PM moving toward the west coast of Greenland at a rate of 6.74 cm/yr (Seo et al., 2021). Figure 4 shows that groundwater depletion is the second largest contributor to the trend in PM excitation. Figure 4b compares observed (red) and estimated (blue) PM excitation trends. The estimated PM excitation trend is the vector sum of all arrows in Figure 4a, additionally including effects of soil moisture, barometric pressure, ocean bottom pressure, winds and currents. Ellipses represent PM excitation rate uncertainties estimated from the sum of squared formal errors in trend estimates at a 95% confidence level. The solid blue and dashed arrows show PM excitation estimates with and without groundwater, respectively. Excluding groundwater, estimated and observed PM excitation trends do not agree well. The difference is greatly reduced when groundwater is included. Observed GMSL rate from multiple satellite altimetry is also closely explained when including groundwater depletion data (see Figure S2 in Supporting Information S1).

All six estimates (combinations of two polar ice sheet and three mountain glacier estimates) are shown as blue circles in Supporting Information S1 (Figure S3). All agree reasonably well with the observed (red arrow). Additionally, two different GIA model predictions (Peltier et al. (2018), green rectangles, and Caron et al. (2018), cyan triangles) are combined with the six estimates. Cyan triangles associated with the GIA prediction of Caron et al. (2018) show PM trends similar to the blue circles. Green rectangles show more westward motion than observed. In any case, by neglecting groundwater, agreement between estimated and observed trends is poorer.

4. Discussion

The various mass redistribution sources in Figure 1 can also be used to predict changes in dynamic oblateness, J_2. J_2 is proportional to the degree 2 zonal coefficient:

$$J_2 = -\sqrt{5}\overline{C_{20}} \tag{3}$$

Figure S4 in Supporting Information S1 shows observed (red) and estimated (blue) J_2 time series from the sum of all sources shown as blue lines in Figure 1 using the GIA prediction of Peltier et al. (2018). Barometric pressure and ocean bottom pressure are also included. Both time series agree well with one another, but

there is some difference in trend. Most high frequency variations are explained by barometric pressure and ocean bottom pressure, as in the case of PM excitation in Figure 3. The black line shows changes in J_2 due to groundwater variations. When compared with Figure 3, it is evident that J_2 is insensitive to groundwater depletion when compared with PM. A negative J_2 trend from groundwater depletion over land (mostly at low latitudes) is largely canceled by the corresponding contribution from sea level rise, so J_2 does not provide a useful constraint on groundwater depletion. In addition, uncertainty in GIA effects on J_2 further limits its utility as a constraint. Figure S5 in Supporting Information S1 summarizes observed and estimated J_2 rates from the sources used in Supporting Information S1 (Figure S4). Adopting the GIA prediction from Peltier et al. (2018), there is a minor trend disagreement between the estimated (red box) and observed (gray horizontal box) J_2 rates. Mitrovica et al. (2015) proposed a modified mantle viscosity profile and re-estimated the GIA J_2 rate (green line). The result is much less than observed. The GIA model of Caron et al. (2018) is based on inversion of vertical motion data (rather than employing an ice history model to predict GIA). It provides a different J_2 rate (blue line), with the resulting sum shown by the blue box, slightly smaller than observed. Because disagreement among the three different GIA J_2 predictions is much larger than the estimated J_2 rate associated with groundwater depletion, J_2 is not, at present, useful in further constraining terrestrial ice/water mass changes and sea level rise.

Previously, a similar PM excitation was estimated based on GRACE data (Adhikari & Ivins, 2016) for 2003–2015. A comparison of PM excitation between this study and the previous study during the common period (2003–2010) would be useful to understand the relative accuracy of the PM excitation estimate here. Figure S6 in Supporting Information S1 shows the two PM excitation time series for 2003–2010. Annual components were removed and effects of winds and currents were not included to be consistent with the previous study. Both time series show very similar variations, but there are some trend discrepancies. Trends in PM excitation (χ_1, χ_2) based on GRACE data were estimated to be 3.27 and 3.43 mas/yr, respectively (Adhikari & Ivins, 2016), compared to 3.63 and 2.49 mas/yr from this study. The minor difference between the two estimates is likely due to some missing information here, with GRACE data included in the previous study.

Storage changes in natural lakes, not considered here, would be a non-negligible source of GMSL and/or PM variations. However, the high variability of many lake levels leaves their contribution to the long-term GMSL trend uncertain (WCRP, 2018). Another difficulty is the lack of a global database for lake level variations, in contrast to one for artificial reservoirs. Mantle convection would be another potential contributor to a PM trend (Adhikari et al., 2018), but have not included this effect due to its large uncertainty. Large earthquakes would also affect the PM trend (Xu & Chao, 2019). The small trend discrepancy (shown in Figure 4) in observed and estimated PM excitations found in this study may be further reconciled by including these effects.

5. Conclusions

Global climate model estimates indicate that groundwater depletion is a significant contributor to GMSL rise. Since the launch of GRACE, observations of time-variable gravity show large amounts of groundwater depletion and resulting sea level rise. Prior to the GRACE mission, GMSL budgets indicated declining groundwater, but confirmation from direct observations was lacking on a global scale. Independent confirmation of groundwater's contribution to GMSL changes might come from variations in Earth's dynamic oblateness (J_2) and polar motion (PM). We found that J_2 is not especially useful for this purpose because of the geography (low latitudes) of aquifers that have been depleted in this period, and uncertainty in GIA predictions regarding J_2. On the other hand, PM excitation, (χ_1, χ_2), for 1993–2010 is sensitive to global groundwater changes, and observed and predicted PM excitations agree well with each other. We found that groundwater depletion was the second largest (4.36 cm/yr) component of PM excitation trend toward 64.16°E during 1993–2010. Among known sources of PM excitation, groundwater changes are particularly important to explain the χ_2 component, trending toward 90° east longitude. Neglecting groundwater depletion in the PM excitation budget leads to a trend that is more westward than observed. Various choices for estimates of other surface mass load contributions lead to the same conclusion. This confirms that groundwater depletion is a major source of GMSL rise during the last a few decades as previously indicated by these models.

Data Availability Statement

The data that support the findings of this study are available from a data repository of Open Science Framework (http://doi.org/10.17605/OSF.IO/S9VHN).

Acknowledgments
This work was supported by the Korea Institute of Marine Science & Technology Promotion (KIMST) grant funded by the Ministry of Ocean Fisheries (RS-2023-00256677; PM23020), and National Research Foundation of Korea (NRF) Grant (No. 2023R1A2C1004899). J.C. is supported by PolyU SHS and LSGI Internal Research Funds, and C.R.W. is supported by NASA Grants 80NSSC22K0906 and 80NSSC20K0820. We appreciate Y. Wada for providing the groundwater depletion model data.

References

Adhikari, S., Caron, L., Steinberger, B., Reager, J. T., Kjeldsen, K. K., Marzeion, B., et al. (2018). What drives 20th century polar motion? *Earth and Planetary Science Letters*, *502*, 126–132. https://doi.org/10.1016/j.epsl.2018.08.059

Adhikari, S., & Ivins, E. R. (2016). Climate-driven polar motion: 2003–2015. *Science Advances*, *2*(4), e1501693. https://doi.org/10.1126/sciadv.1501693

Bizouard, C., Lambert, S., Gattano, C., Becker, O., & Richard, J.-Y. (2019). The IERS EOP 14C04 solution for Earth orientation parameters consistent with ITRF 2014. *Journal of Geodesy*, *93*(5), 621–633. https://doi.org/10.1007/s00190-018-1186-3

Caron, L., Ivins, E. R., Larour, E., Adhikari, S., Nilsson, J., & Blewitt, G. (2018). GIA model statistics for GRACE hydrology, cryosphere, and ocean science. *Geophysical Research Letters*, *45*(5), 2203–2212. https://doi.org/10.1002/2017gl076644

Chao, B. F. (1985). On the excitation of the Earth' polar motion. *Geophysical Research Letters*, *12*(8), 526–529. https://doi.org/10.1029/gl012i008p00526

Chao, B. F., Wu, Y. H., & Li, Y. S. (2008). Impact of artificial reservoir water impoundment on global sea level. *Science*, *320*(5873), 212–214. https://doi.org/10.1126/science.1154580

Chen, J. L., Wilson, C. R., Ries, J. C., & Tapley, B. D. (2013). Rapid ice melting drives Earth's pole to the east. *Geophysical Research Letters*, *40*(11), 2625–2630. https://doi.org/10.1002/grl.50552

Chen, J. L., Wilson, C. R., & Tapley, B. D. (2013). Contribution of ice sheet and mountain glacier melt to recent sea level rise. *Nature Geoscience*, *6*(7), 549–552. https://doi.org/10.1038/ngeo1829

Deng, S., Liu, S., Mo, X., Jiang, L., & Bauer-Gottwein, P. (2021). Polar drift in the 1990s explained by terrestrial water storage changes. *Geophysical Research Letters*, *48*(7), e2020GL092114. https://doi.org/10.1029/2020gl092114

Dieng, H. B., Cazenave, A., Meyssignac, B., & Ablain, M. (2017). New estimate of the current rate of sea level rise from a sea level budget approach. *Geophysical Research Letters*, *44*(8), 3744–3751. https://doi.org/10.1002/2017gl073308

Hersbach, H., Bell, B., Berrisford, P., Hirahara, S., Horányi, A., Muñoz-Sabater, J. et al. (2020). The ERA5 global reanalysis. *Quarterly Journal of the Royal Meteorological Society*, *146*, 1999–2049. https://doi.org/10.1002/qj.3803

Jeon, T., Seo, K.-W., Youm, K., Chen, J., & Wilson, C. R. (2018). Global sea level change signatures observed by GRACE satellite gravimetry. *Scientific Reports*, *8*(1), 13519. https://doi.org/10.1038/s41598-018-31972-8

Kim, J.-S., Seo, K.-W., Jeon, T., Chen, J., & Wilson, C. R. (2019). Missing hydrological contribution to sea level rise. *Geophysical Research Letters*, *46*(21), 12049–12055. https://doi.org/10.1029/2019gl085470

Köhl, A. (2020). Evaluating the GECCO3 1948–2018 ocean synthesis—A configuration for initializing the MPI-ESM climate model. *Quarterly Journal of the Royal Meteorological Society*, *146*(730), 2250–2273. https://doi.org/10.1002/qj.3790

Lehner, B., Liermann, C. R., Revenga, C., Vörösmarty, C., Fekete, B., Crouzet, P., et al. (2011). High-resolution mapping of the world's reservoirs and dams for sustainable river-flow management. *Frontiers in Ecology and the Environment*, *9*(9), 494–502. https://doi.org/10.1890/100125

Marzeion, B., Leclercq, P. W., Cogley, J. G., & Jarosch, A. H. (2015). Brief communication: Global reconstructions of glacier mass change during the 20th century are consistent. *The Cryosphere*, *9*(6), 2399–2404. https://doi.org/10.5194/tc-9-2399-2015

Mitrovica, J. X., Hay, C. C., Morrow, E., Kopp, R. E., Dumberry, M., & Stanley, S. (2015). Reconciling past changes in Earth's rotation with 20th century global sea-level rise: Resolving Munk's enigma. *Science Advances*, *1*(11), e1500679. https://doi.org/10.1126/sciadv.1500679

Mouginot, J., Rignot, E., Bjørk Anders, A., van den Broeke, M., Millan, R., Morlighem, M., et al. (2019). Forty-six years of Greenland Ice Sheet mass balance from 1972 to 2018. *Proceedings of the National Academy of Sciences of the United States of America*, *116*(19), 9239–9244. https://doi.org/10.1073/pnas.1904242116

Peltier, W. R., Argus, D. F., & Drummond, R. (2018). Comment on "An assessment of the ICE-6G_C (VM5a) glacial isostatic adjustment model" by Purcell et al. *Journal of Geophysical Research: Solid Earth*, *123*(2), 2019–2028. https://doi.org/10.1002/2016jb013844

Reager, J. T., Gardner, A. S., Famiglietti, J. S., Wiese, D. N., Eicker, A., & Lo, M. H. (2016). A decade of sea level rise slowed by climate-driven hydrology. *Science*, *351*(6274), 699–703. https://doi.org/10.1126/science.aad8386

Rignot, E., Mouginot, J., Scheuchl, B., van den Broeke, M., van Wessem Melchior, J., & Morlighem, M. (2019). Four decades of Antarctic Ice Sheet mass balance from 1979–2017. *Proceedings of the National Academy of Sciences of the United States of America*, *116*(4), 1095–1103. https://doi.org/10.1073/pnas.1812883116

Rodell, M., Famiglietti, J. S., Chen, J., Seneviratne, S. I., Viterbo, P., Holl, S., & Wilson, C. R. (2004). Basin scale estimates of evapotranspiration using GRACE and other observations. *Geophysical Research Letters*, *31*(20), L20504. https://doi.org/10.1029/2004gl020873

Seo, K.-W., Kim, J.-S., Youm, K., Chen, J., & Wilson, C. R. (2021). Secular polar motion observed by GRACE. *Journal of Geodesy*, *95*(4), 40. https://doi.org/10.1007/s00190-021-01476-x

The IMBIE Team. (2018). Mass balance of the Antarctic Ice Sheet from 1992 to 2017. *Nature*, *558*(7709), 219–222. https://doi.org/10.1038/s41586-018-0179-y

The IMBIE Team. (2020). Mass balance of the Greenland Ice Sheet from 1992 to 2018. *Nature*, *579*(7798), 233–239. https://doi.org/10.1038/s41586-019-1855-2

Wada, Y., van Beek, L. P. H., van Kempen, C. M., Reckman, J. W. T. M., Vasak, S., & Bierkens, M. F. P. (2010). Global depletion of groundwater resources. *Geophysical Research Letters*, *37*(20), L20402. https://doi.org/10.1029/2010gl044571

Wada, Y., van Beek, L. P. H., Viviroli, D., Dürr, H. H., Weingartner, R., & Bierkens, M. F. P. (2011). Global monthly water stress: 2. Water demand and severity of water stress. *Water Resources Research*, *47*(7), W07518. https://doi.org/10.1029/2010wr009792

WCRP. (2018). Global sea-level budget 1993–present. *Earth System Science Data*, *10*(3), 1551–1590. https://doi.org/10.5194/essd-10-1551-2018

Wilson, C. R. (1985). Discrete polar motion equations. *Geophysical Journal of the Royal Astronomical Society*, *80*(2), 551–554. https://doi.org/10.1111/j.1365-246x.1985.tb05109.x

Xu, C. Y., & Chao, B. F. (2019). Seismic effects on the secular drift of the Earth's rotational pole. *Journal of Geophysical Research: Solid Earth*, *124*. https://doi.org/10.1029/2018JB017164

Zemp, M., Huss, M., Thibert, E., Eckert, N., McNabb, R., Huber, J., et al. (2019). Global glacier mass changes and their contributions to sea-level rise from 1961 to 2016. *Nature*, *568*(7752), 382–386. https://doi.org/10.1038/s41586-019-1071-0